Effect of microstructure on the stability of retained austenite in transformation-induced-plasiticity steels

I B. Timokhina
Monash University, Ilana.Timokhina@eng.monash.edu.au

P D. Hodgson
Deakin University

E V. Pereloma
University of Wollongong, elenap@uow.edu.au

Effect of microstructure on the stability of retained austenite in transformation-induced-plasiticity steels

Abstract

Two Fe-0.2C-1.55Mn-1.5Si (in wt pct) steels, with and without the addition of 0.039Nb (in wt pct), were studied using laboratory rolling-mill simulations of controlled thermomechanical processing. The microstructures of all samples were characterized by optical metallography, X-ray diffraction (XRD), and transmission electron microscopy (TEM). The microstructural behavior of phases under applied strain was studied using a heat-tinting technique. Despite the similarity in the microstructures of the two steels (equal amounts of polygonal ferrite, carbide-free bainite, and retained austenite), the mechanical properties were different. The mechanical properties of these transformation-induced-plasticity (TRIP) steels depended not only on the individual behavior of all these phases, but also on the interaction between the phases during deformation. The polygonal ferrite and bainite of the C-Mn-Si steel contributed to the elongation more than these phases in the C-Mn-Si-Nb-steel. The stability of retained austenite depends on its location within the microstructure, the morphology of the bainite, and its interaction with other phases during straining. Granular bainite was the bainite morphology that provided the optimum stability of the retained austenite.

Keywords

stability, retained, effect, microstructure, austenite, steels, plasiticity, induced, transformation

Disciplines

Engineering | Science and Technology Studies

Effect of Microstructure on the Stability of Retained Austenite in Transformation-Induced-Plasticity Steels

I.B. TIMOKHINA, P.D. HODGSON, and E.V. PERELOMA

Two Fe-0.2C-1.55Mn-1.5Si (in wt pct) steels, with and without the addition of 0.039Nb (in wt pct), were studied using laboratory rolling-mill simulations of controlled thermomechanical processing. The microstructures of all samples were characterized by optical metallography, X-ray diffraction (XRD), and transmission electron microscopy (TEM). The microstructural behavior of phases under applied strain was studied using a heat-tinting technique. Despite the similarity in the microstructures of the two steels (equal amounts of polygonal ferrite, carbide-free bainite, and retained austenite), the mechanical properties were different. The mechanical properties of these transformation-induced-plasticity (TRIP) steels depended not only on the individual behavior of all these phases, but also on the interaction between the phases during deformation. The polygonal ferrite and bainite of the C-Mn-Si steel contributed to the elongation more than these phases in the C-Mn-Si-Nb-steel. The stability of retained austenite depends on its location within the microstructure, the morphology of the bainite, and its interaction with other phases during straining. Granular bainite was the bainite morphology that provided the optimum stability of the retained austenite.

I. INTRODUCTION

THE introduction of new types of steels in the automotive industry, such as *transformation-induced-plasticity* (TRIP) steels, has been driven by the requirements to increase the ductility without compromising the strength. The TRIP steels offer a unique combination of ultimate tensile strength (~1000 MPa) and elongation (up to 40 pct).[1] The microstructure of these steels consists of polygonal ferrite, bainite, retained austenite (~10 to 20 pct), and martensite.[2] The main phenomenon responsible for the improved mechanical properties has been proposed to be the deformation-induced transformation of the metastable retained austenite to martensite during straining.[3,4] Based on this, most of the past research has concentrated on the relationships between the volume fraction and stability of the retained austenite and the mechanical properties.[5–9] It has been reported that an increase in the volume fraction of retained austenite increases the strain-hardening coefficient, which leads to an increase in elongation.[5,6,7] On the other hand, a number of articles have shown that a higher amount of retained austenite does not necessarily result in a higher uniform elongation, because the higher amount of retained austenite may have a lower average carbon content, leading to low stability during deformation. Hence, there is an optimum amount of the retained austenite required to increase the elongation of TRIP steels.[8,9]

The main parameters that can dictate the stability of the retained austenite during deformation are the carbon content, size, morphology, and distribution within the microstructure. The carbon content determines the chemical driving force for the transformation of retained austenite to martensite, the stress-free transformation strain (through its influence on the lattice parameter), and the flow behavior of the retained austenite.[10] It has recently been reported that retained austenite with a low carbon content (<0.5 to 0.6 wt pct) transforms to martensite more rapidly during plastic straining and does not contribute to an increase in elongation.[11] On the other hand, a much higher carbon content (>1.8 wt pct) results in the incomplete transformation of the retained austenite to martensite after deformation and also does not lead to an increase in elongation.[12] Recent research has also shown that retained-austenite grains larger than 1-μm are unstable and do not contribute significantly to the ductility of the material,[13] since smaller retained-austenite crystals contain less potential nucleation sites for the transformation to martensite and, consequently, require a greater total driving force for the nucleation of martensite.[9] On the other hand, the retained-austenite islands, which are smaller than submicron size, have a low tendency to transform to martensite, even if necking occurs, and, thus, do not contribute to the ductility.[14,15]

The morphology of the retained austenite is also important for the stabilization. The best elongation behavior has been observed when the retained austenite is present as films between the subunits of bainite, rather than as blocky regions between sheaves of bainitic ferrite.[16,17] The blocks of austenite tend to transform to martensite under a small strain and, consequently, do not contribute to the TRIP effect.[16] The kinetics of the deformation-induced transformation can also be affected by the location of the retained austenite in the microstructure. According to Tsukatani *et al.*,[18] the presence of the martensite in the vicinity of retained austenite diminishes the TRIP effect because martensite propagates stress directly to the retained austenite, which may then easily transform to martensite at an early stage of straining.[18] Bainitic ferrite can also act as a barrier against the autocatalytic propagation of the $\gamma \rightarrow \alpha'$ transformation.[7]

I.B. TIMOKHINA, formerly Postdoctoral Student, School of Engineering and Technology, Deakin University, is Research Associate, School of Physics and Materials Engineering, Monash University. Contact e-mail: ilana.timokhina@spme.monash.edu.au P.D. HODGSON, Alfred Deakin Professor and Associate Dean, is with the School of Engineering and Technology, Deakin University, Geelong, VIC 3217, Australia. E.V. PERELOMA, Senior Lecturer, is with the School of Physics and Materials Engineering, Monash University, VIC 3800, Australia.

Recent publications have also revealed the importance of the effect of polygonal ferrite and the interaction between polygonal ferrite, retained austenite, and strain-induced martensite during straining on the structure-property relationship in TRIP steels.[19,20,21] However, since the TRIP steel microstructure also contains bainites with different morphologies, it is proposed that the effect of the interaction of all phases present in the microstructure on the microstructure-property relationship should also be considered.

The key objective of this work, therefore, is to study the stability of the retained austenite during deformation and to understand the contribution of polygonal ferrite, bainite, and the interaction between the different phases in the microstructure and the mechanical properties of thermomechanically processed TRIP steels.

II. EXPERIMENTAL

Two experimental C-Mn-Si steels, with and without the addition of Nb (Table I), were studied. These steels were received in the as-rolled plate condition from BHP Research–Melbourne Laboratories.

A laboratory rolling mill was used to simulate full-scale rolling. The thermomechanical processing schedules were constructed, based on the analyses of the continuous cooling–transformation data, to form the microstructures with 50 pct of polygonal ferrite and carbide-free bainite to stabilize the maximum volume fraction of the retained austenite to room temperature. The samples were reheated in a 15 kW muffle furnace and soaked for 120 seconds at the temperature of 1523 K (Figure. 1). After the soak time, the samples were pushed immediately through the rolling mill at 1373 K, where the first deformation ($\varepsilon_1 = 0.25$) took place followed by a 120-second hold to achieve a uniform, recrystallized austenite grain structure. Then, the samples were cooled at $\sim$2 Ks^{-1} and subjected to the second deformation ($\varepsilon_2 = 0.47$) at 1098 K (non-Nb steel) and 1123 K (Nb steel). After the second deformation, specimens were cooled at $\sim$1 Ks^{-1} to 943 K, to form $\sim$50 to 60 pct of polygonal ferrite. Two spray guns were used to cool the specimen at $\sim$20 Ks^{-1} to 773 K. At this point, the samples were lowered into a fluidbed furnace and covered with aluminum oxide sand to hold the sample at a 723 K coiling temperature for 600 seconds. After holding, the samples were quenched in an iced brine solution. The final thickness was $\sim$6.5 mm.

The microstructures of the specimens were characterized using optical metallography and transmission electron microscopy (TEM). Specimens were sectioned parallel to the deformation direction for optical metallography, while thin foils for TEM study were cut perpendicular to the deformation direction. The specimen preparation for optical examination involved standard metallographic procedures. These samples were etched with 2 pct Nital to reveal the microstructure. Micrographs were taken along the deformation direc-

tion from the center of the specimens. Thin foils were prepared by twin-jet electropolishing using a solution of 5 pct perchloric acid in methanol at 253 K and an operating voltage of 30 V. Bright-field and dark-field images and selected-area electron diffraction patterns were obtained using a PHILIPS* CM20 microscope operated at 200 kV.

---

*PHILIPS is a trademark of Philips Electronic Instruments Corp. Mahwah, NJ.

To investigate the NbC precipitation, the TEM replicas from the quenched samples after the deformations in the recrystallized and nonrecrystallized austenite regions were studied using bright-field image TEM and energy-dispersive X-ray spectroscopy analysis.

Room-temperature mechanical properties were determined using an Instron 4500 servohydraulic tensile-testing machine with a 100 kN load cell. The crosshead speed was fixed at 0.5 mm/min. Subsize samples with a 25 mm gage length and 6 mm thickness were used to minimize the amount of material.[22]

The strain-hardening coefficient (n) was calculated from the stress-strain data using the following equation:[23]

$$n = \frac{d(\ln \sigma)}{d(\ln \varepsilon)} \quad [1]$$

where σ is the true stress and ε is the true strain.

The stability of retained austenite and the transformation behavior of phases, as a function of the plastic strain, was studied on the samples after tensile testing using a heat-tinting technique and TEM investigation. The samples after straining were cut along the longitudinal direction and perpendicular to the deformation direction into 3-mm-thick slices. Three dimensions (l = length, t = thickness, and w = width) of these small sections were measured before and
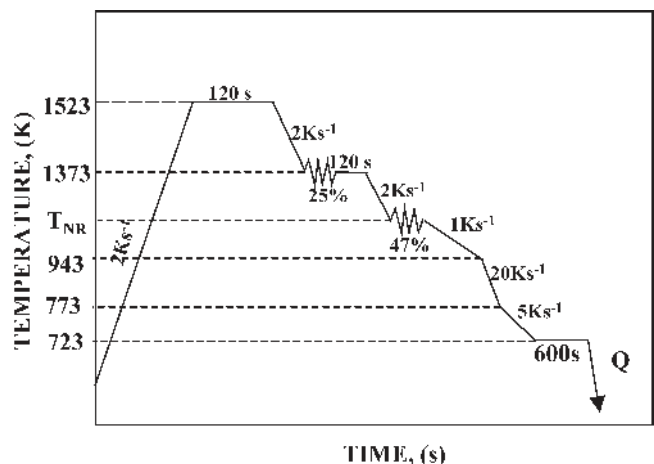

Fig. 1—Thermomechanical processing schedule.

Table I. Chemical Composition of Steels, Weight Percent

Steel	C	Mn	Si	Ni	Mo	Cu	Nb	Ti	N
Nb steel	0.21	1.51	1.49	—	0.004	0.02	0.039	<0.05	0.0007
Non-Nb steel	0.21	1.55	1.55	0.009	≤0.008	0.003	0.005	≤0.003	0.0035

after tensile tests to define the equivalent of strain, using the following empirical equation:[23]

$$\varepsilon = \frac{\sqrt{2}}{3}\sqrt{(\varepsilon_t - \varepsilon_l)^2 + (\varepsilon_t - \varepsilon_w)^2 + (\varepsilon_l - \varepsilon_w)^2} \quad [2]$$

where $\varepsilon_t = \ln(t_1/t_o)$, $\varepsilon_l = \ln(l_1/l_o)$, and $\varepsilon_w = \ln(w_1/w_o)$.

After that, the TEM samples were prepared from these sections to study the retained-austenite stability.

The heat-tinting technique was used to distinguish austenite and martensite.[24] An unmounted sample was polished and etched with 2 pct Nital for about 15 seconds. After that, the sample was heated in a furnace in air at ~533 K for 2.5 hours, without a protective atmosphere, then cooled to room temperature. With this technique, the various phases appear as different colors under the microscope. Polygonal ferrite and bainitic ferrite are beige, retained austenite is purple, and martensite is dark blue. This method provides the opportunity to observe the changes in the retained-austenite/martensite volume fraction, distribution, and size during tensile testing. Scanning electron microscopy and X-ray analysis were carried out on the samples before and after the heat-tinting technique to ensure that the heat treatment, used in the heat tinting, did not affect the volume fraction and the stability of the retained austenite. The volume fraction of retained austenite obtained from the X-ray data was similar to that after the heat-tinting technique. Quantitative analysis of retained austenite and martensite after heat tinting was accomplished using image-analysis software.

An X-ray diffraction (XRD) analysis was carried out using a PHILIPS PW 1130 (40 kV, 30 mA) diffractometer equipped with a monochromator and Cu K_α radiation to confirm the amount of martensite and retained austenite formed in the microstructure. Spectra were taken in the range of 2θ from 30 to 90 deg, with a 0.5 deg step size. The integrated intensities of the $(200)_\alpha$, $(211)_\gamma$, $(200)_\gamma$, and $(220)_\gamma$ peaks were used in the direct comparison method[25] to determine the volume fraction of retained austenite in the rolled samples and in each section of the tensile specimens with different amounts of strain. The XRD data were also used to calcu-

late the carbon concentration in the retained-austenite lattice using the following equation:[26]

$$a_\gamma = (0.363067 + 0.0783/(1 + 0.2151$$
$$(100/\text{wt pct C} - 1))) \times (1 + (24.92 - 51/(1 + 0.2151$$
$$(100/\text{wt pct C} - 1)))) \times 10^{-6}(T - 727) \quad [3]$$

An estimation of the contribution of the polygonal ferrite and bainite present in the microstructure to the total elongation of steels was based on the calculation of the individual strain of these phases at different strains. The strains of the individual phases were determined using the linear-intercept method along three (longitudinal, transverse, and perpendicular) directions of each section, with 20 intercepts/measurement before and after tensile tests. The calculations of the bainite strain included the contribution of the strain-induced transformation of the retained austenite. After that, the strains of the phases were calculated using Eq. [2].

III. RESULTS

A. Microstructure and Properties of Steels after Thermomechanical Processing

The microstructures (Figure 2) formed after laboratory rolling were similar for both steels, consisting of 50 to 55 pct polygonal ferrite, carbide-free bainitic phases (granular bainite and acicular ferrite), and 14 pct retained austenite and martensite. Granular bainite is characterized by the absence of carbides and the presence of isolated regions of retained austenite and martensite between crystals of bainitic ferrite, which have a grain or plate morphology (Figure 3(a)). The acicular ferrite structure appeared to be a bainitic structure with retained-austenite and martensite layers between the bainitic ferrite laths (or lenticular plates) (Figure 3(b)). The retained austenite of both steels was observed in five main morphologies: (1) blocky islands between polygonal ferrite grains (Figure 3(c)), (2) islands at the polygonal ferrite/bainite interface (Figure 3(d)), (3) islands in granular bainite (Figure 3(a)),
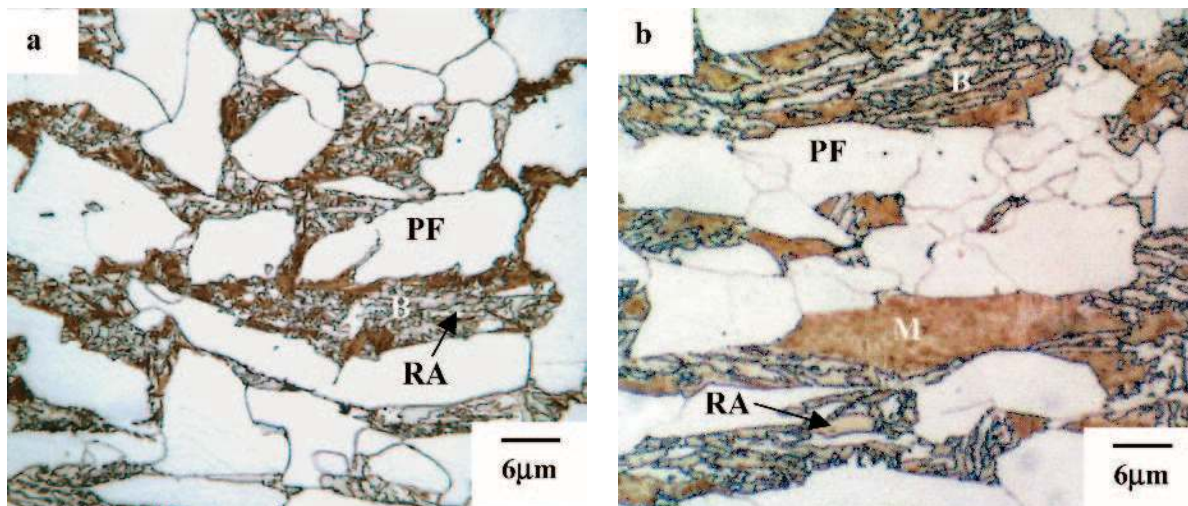

Fig. 2—Optical micrographs of the Nital-etched (*a*) non-Nb and (*b*) Nb-steel samples after thermomechanical processing (PF is polygonal ferrite, M is martensite, RA is retained austenite, and B is bainite).
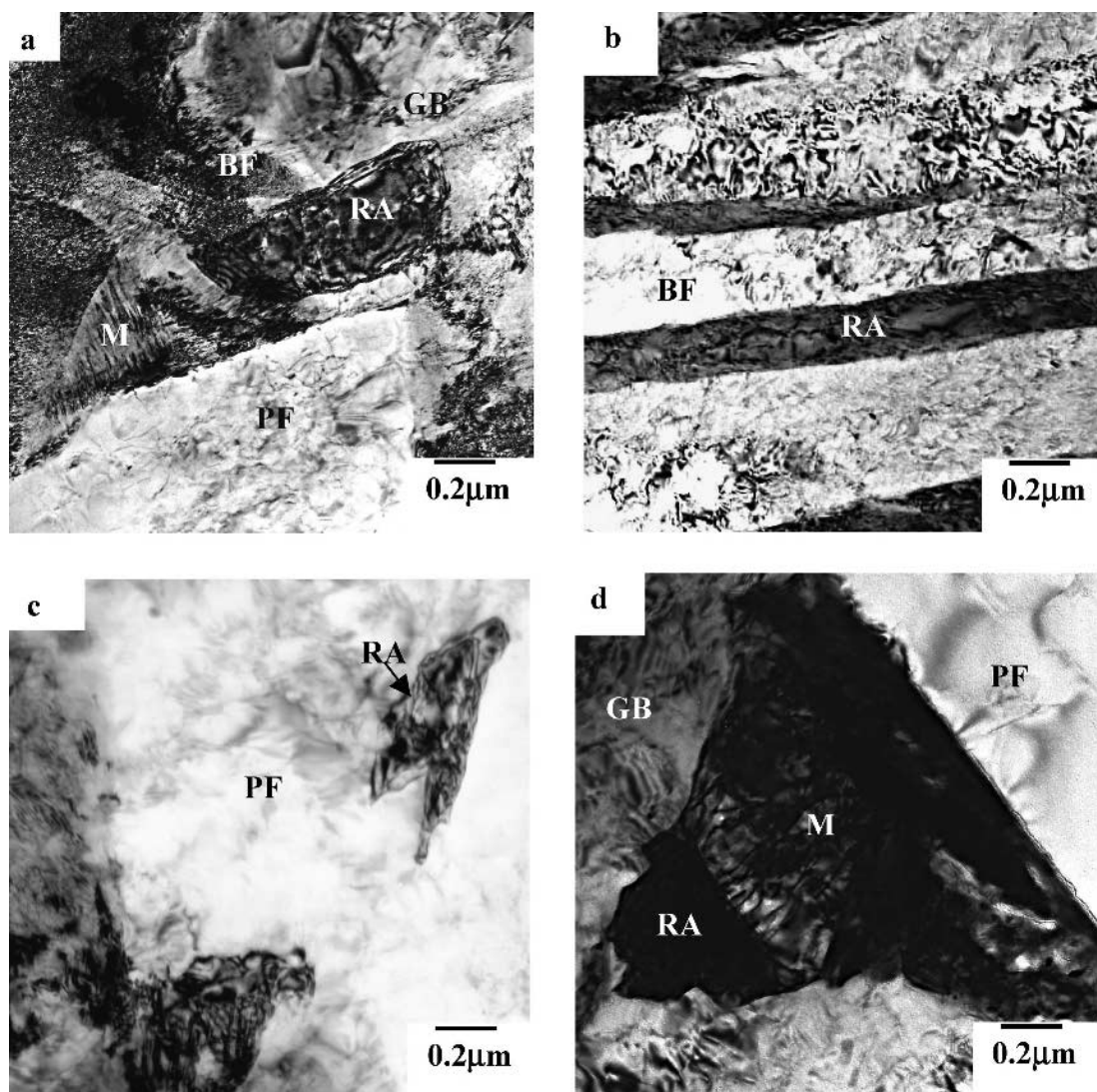
Fig. 3—Thin-foil TEM microstructures of (*a*) island of retained austenite in granular bainite, (*b*) acicular ferrite with interlayers of retained austenite, (*c*) retained austenite in polygonal ferrite, and (*d*) martensite/retained austenite constituent. PF is polygonal ferrite, BF is bainitic ferrite, GB is granular bainite, RA is retained austenite, and M is martensite.

and (4) films or layers between acicular ferrite laths (Figure 3(b)) and (5) the retained-austenite/martensite constituent (Figure 3(d)).

The microstructural analyses of the samples revealed that the polygonal ferrite grain size of the non-Nb steel was 13.0 ± 2.6 μm in thickness, while the ferrite grain thickness in the Nb steel was 9.0 ± 1.9 μm (Figure 2). The refinement of the polygonal ferrite grains appeared to be due to the formation of the NbC particles in the microstructures of Nb steel (Figure 4). These particles displayed a globular or cubic form and were observed within the matrix and at the grain boundaries. The average size of the carbides was 25 ± 10 nm. The Nb steel appeared to have a higher amount of acicular ferrite, while granular bainite was the dominant bainitic phase in the non-Nb steel. The martensite islands in the Nb steel were coarse, with a slightly higher volume fraction than in the non-Nb steel (Figure 2, Table II). Moreover, the amount of retained austenite between the polygonal ferrite grains and at the bainite/polygonal ferrite interface was higher by

about 10 pct in the microstructure of the Nb steel than in the non-Nb steel.

Despite the microstructural refinement and the similar amount of retained austenite in the microstructure of both steels, the non-Nb steel exhibited a better combination of mechanical properties; in particular, the non-Nb steels had the higher value of ultimate tensile strength with a higher value of uniform elongation (Figure 5, Table II). The microstructural dissimilarity between two steels led to the difference in yield strength. The Nb steel demonstrated a higher value than the non-Nb steel (Figure 5, Table II).

The study of strain-hardening variation also revealed the difference in the microstructural behavior during straining for two steels (Figure 6). The strain-hardening coefficient for the non-Nb steel gradually reached a maximum (0.30) at a strains of ~0.08 and ~0.22, demonstrated almost steady behavior during further straining, and then decreased continuously (Figure 6). The n value for the Nb steel increased steeply to a maximum (~0.165) at the beginning of straining

and then exhibited a gradual decrease during further straining (Figure 6). A more gradual behavior of the strain-hardening curve correlated with the higher uniform elongation in the non-Nb steel.
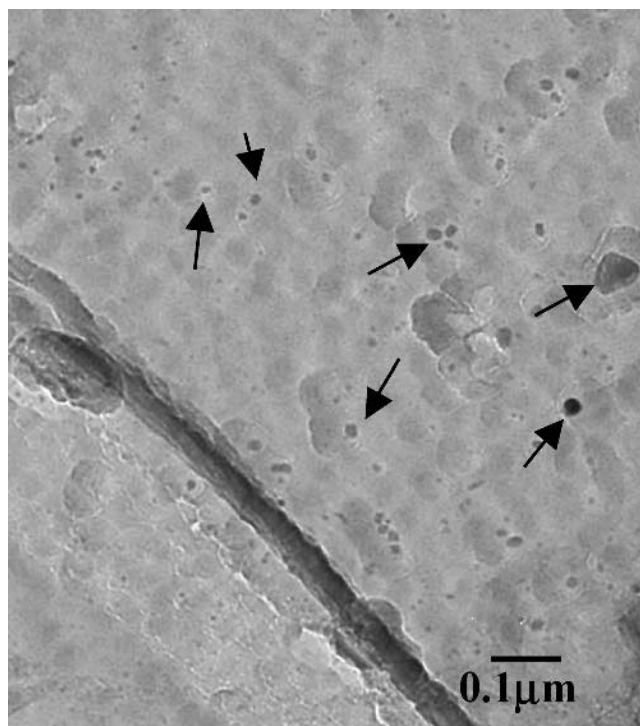
(a)
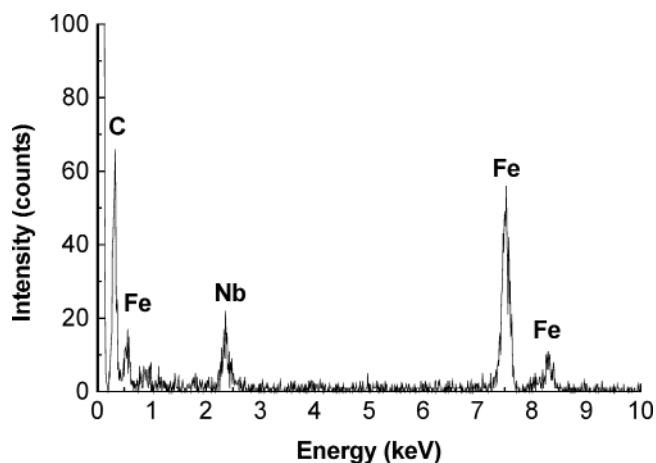
(b)

Fig. 4—TEM replica micrograph and EDXS spectra of NbC particles.

B. *Microstructural Behavior under Applied Strain*

The heat-tinting technique was used to reveal the different behaviors of the phases in the two steels during tensile deformation, as this technique allowed local analysis of the phases. Metallographic observation of the non-Nb steel and Nb steel tensile samples after heat tinting at several levels of strain exposed the differences in the microstructural evolution for the non-Nb and Nb steels (Figure 7). Although the samples contained similar amounts of retained austenite, the rate of the retained-austenite transformation during plastic straining was more gradual in the non-Nb steel (Figure 8).
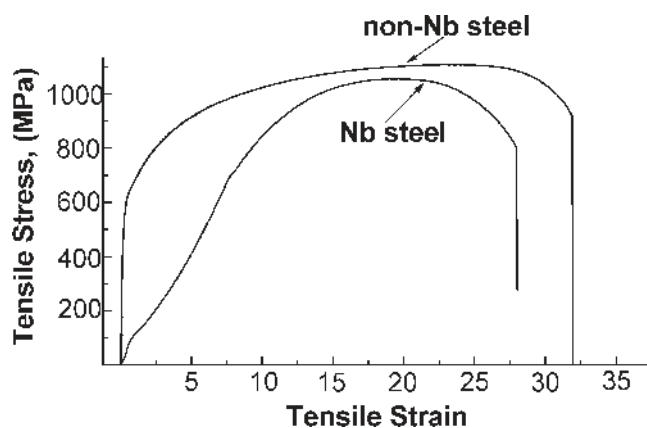

Fig. 5—An example of stress-strain curve for the non-Nb and Nb steels.
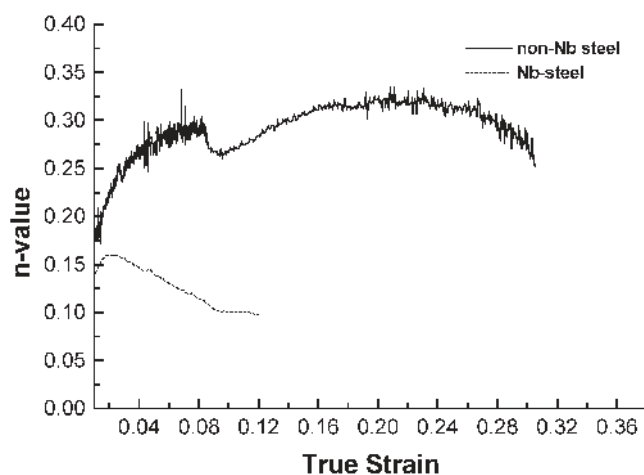
Fig. 6—An example of strain-hardening coefficient behavior with true strain for the non-Nb and Nb steels.

Table II. Mechanical Properties and Volume Fractions of Retained Austenite and Martensite in the Samples after Thermomechanical Processing

Steels	UTS, (MPa)	Yield Strength, (MPa)	Total Elongation, (Pct)	Uniform Elongation, (Pct)	RA, (Pct)	Martensite, (Pct)	Carbon Content of RA (Wt Pct)
Non-Nb steel	970 ± 50	530 ± 50	43 ± 8	28 ± 5	14 ± 2	6 ± 2	1.8
Nb steel	960 ± 50	700 ± 50	26 ± 5	14 ± 5	14 ± 2	9 ± 2	1.6

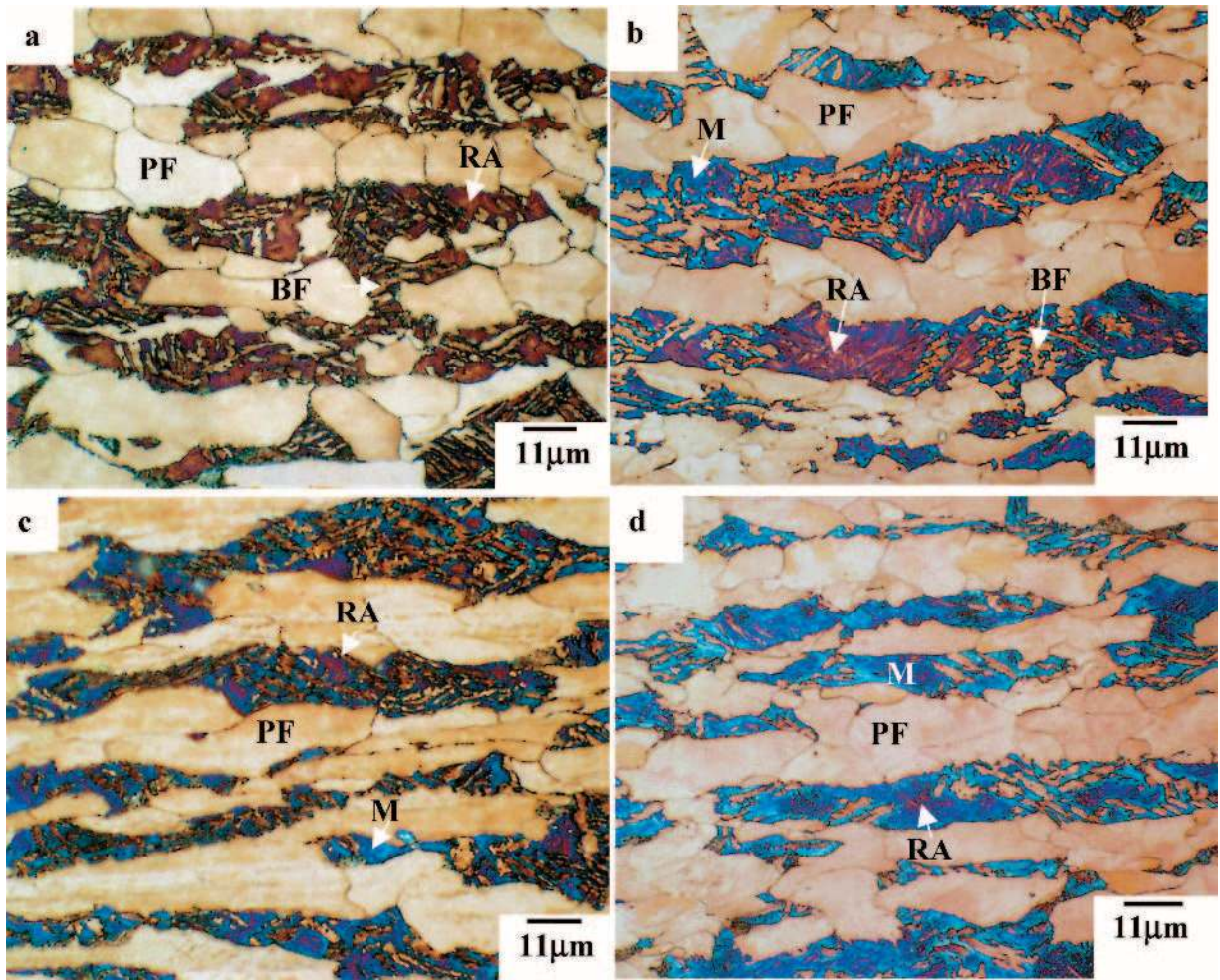Fig. 7—Heat-tinted microstructures of the (*a*) and (*c*) non-Nb steel and (*b*) and (*d*) Nb steel: (*a*) and (*b*) before testing and (*c*) and (*d*) after 0.2 strain (PF is polygonal ferrite, RA is retained austenite, M is martensite, and BF is bainitic ferrite).
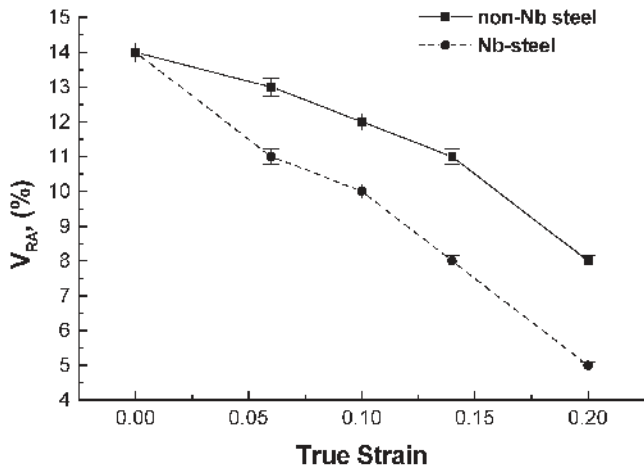

Fig. 8—Volume fraction of retained austenite at different strains.

Examination of the microstructures of the non-Nb and Nb steels during straining revealed that the rate of retained-austenite transformation during straining was affected by its location within the microstructure. The retained-austenite crystals between the polygonal ferrite grains and at the bai-nite/polygonal ferrite interface transformed to martensite at early straining for both steels (Table III). However, deformation in the Nb steel led to a rapid decrease in the amount of retained-austenite crystals at these locations, while the non-Nb steel demonstrated a more gradual decrease in the amount of retained austenite (Table III). Despite this, TEM investigation revealed some of the untransformed, coarse blocks of retained austenite in polygonal ferrite and at the polygonal ferrite/bainite interface in the microstructure after a 0.14 strain (Figure 9(a)). Furthermore, some of the retained-austenite crystals at the polygonal ferrite/bainite interface showed partial transformation to martensite (Figure 9(b)).

It was also found that the kinetic of the retained-austenite transformation during testing was affected by the morphology of the bainitic ferrite. The retained austenite formed between coarse, long, parallel bainitic ferrite laths transformed to martensite at an earlier stage of deformation than those located within granular bainite. Moreover, the regions of retained-austenite crystals located in close proximity to the bainitic ferrite laths transformed faster than the areas in the middle of the austenite crystal (Figure 9(c)). The retained austenite between the refined bainitic ferrite laths appeared to be overstabilized and was observed in the microstructure of the Nb steel even after fracture (Figure 9(d)). The retained

Table III. The Distribution of the Retained Austenite within the Microstructure of the Steels at Different Amount of Strain, Percent (BF is Bainitic Ferrite, PF is Polygonal Ferrite)

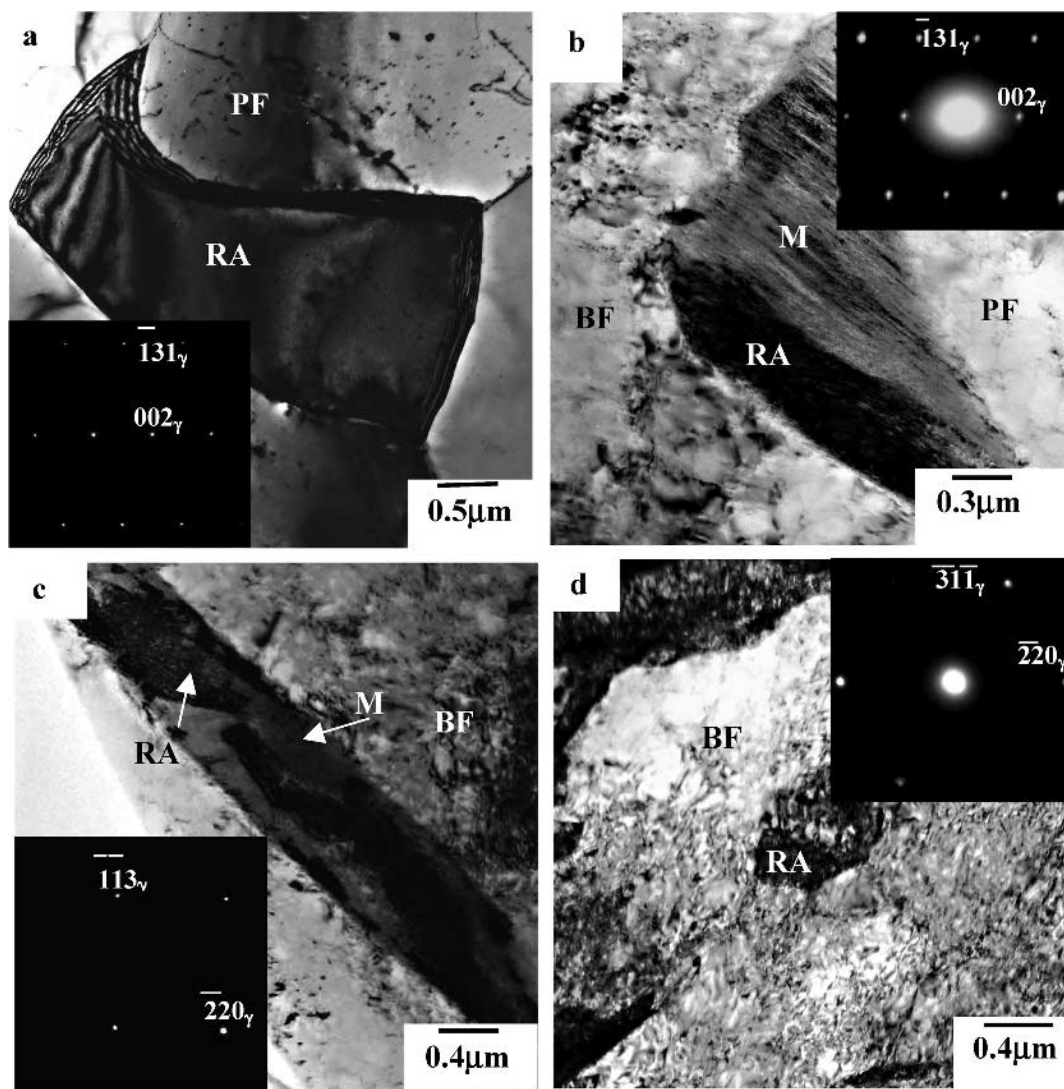| | Strain, (ε) | | | | | | | |
| | 0-0.06 | | 0.1 | | 0.14 | | 0.2 | |
Location	Non-Nb	Nb	Non-Nb	Nb	Non-Nb	Nb	Non-Nb	Nb
RA between BF, pct	~80	~70	~85	~90	~90	~95	~95	~99
RA on PF/Bainite Interface, pct	~18	~25	~15	~10	~10	~5	~5	<1
RA between PF, pct	~2	~5	0	<1	0	<1	0	0
Total amount of RA, pct	13	11	12	10	11	8	8	5
Total amount of martensite, pct	8	13	9	14	10	15	12	18

Fig. 9—Thin-foil TEM microstructures of (*a*) retained austenite in polygonal ferrite after 0.14 strain (zone axis is $[310]_\gamma$), (*b*) retained austenite/martensite constituent after 0.1 (zone axis is $[332]_\gamma$), (*c*) retained austenite after 0.2 strain (zone axis is $[114]_\gamma$), and (*d*) partial transformation of retained austenite (zone axis is $[310]_\gamma$).

austenite between the bainitic ferrite grains in the granular bainite demonstrated the optimum stability, with a gradual transformation to martensite during deformation.

While the transformation of the retained austenite started at an early stage of straining, the deformation of the polygonal ferrite was not evident for strains below $\sim\varepsilon = 0.14$ for both steels. Optical examination of the longitudinal section

of the non-Nb steel after tensile testing showed that after a 0.14 strain, the deformation was concentrated in the polygonal ferrite matrix, causing it to flow around the bainite islands, leading to an elongation of the polygonal ferrite. The polygonal ferrite grains elongated by 47 pct at 0.14 strain and 95 pct at 0.2 strain in the non-Nb steel. The Nb steel demonstrated a different polygonal ferrite behavior.

The polygonal ferrite grains were subdivided into subgrains, but did not flow around the bainite regions (Figures 7(c) and (d)). The polygonal ferrite grains of the Nb steel elongated by 35 and 50 pct at 0.14 and 0.2 strains, respectively.

The behavior of the bainite phase varied in both steels. In the non-Nb steel, the concentration of strain in the bainitic ferrite led to flow of the bainitic ferrite laths around the hard martensite/retained-austenite islands and to their elongation along the deformation direction (Figures 7(c) and (d)), while the Nb steel did not demonstrate this effect. The calculated elongation of the bainite in the non-Nb steel was 14 and 75 pct at 0.14 and 0.2 strains, respectively. In contrast, the bainite in the Nb steel elongated by only 10 pct at a 0.14 strain and 20 pct at a 0.18 strain.

IV. DISCUSSION

A. Morphology, Distribution, and Stability of Retained Austenite

The multiphase microstructure formed in all samples after thermomechanical processing controls the combination of strength and ductility. While the presence of martensite increases strength, a significant amount of polygonal ferrite and retained austenite leads to high values of elongation. It is generally accepted that a higher volume fraction of retained austenite improves elongation due to the strain-induced transformation during deformation. In the present work, the volume fractions of polygonal ferrite, bainite, and retained austenite were similar for both steels. However, the C-Mn-Si TRIP steel showed a better combination of strength and ductility than the C-Mn-Si-Nb steel. This was somewhat surprising, considering that the C-Mn-Si-Nb steel had a more refined microstructure and a higher volume fraction of acicular ferrite with interlayers of retained austenite present, which is considered to be the most favorable morphology for providing the TRIP effect.[27] It is suggested that not only the retained-austenite morphology and carbon content, size, and distribution of retained austenite in the microstructure are responsible for this difference between the two steels, but also the deformation behavior of other phases present in the microstructure and also their interactions.

One of the major factors responsible for the retained-austenite stability is its carbon content, which is affected by the retained-austenite distribution within the microstructure. Despite the similar amount of retained austenite and the more refined bainitic structure in the Nb steel, the average carbon content in the non-Nb steel was higher (1.8 wt pct) compared to the Nb steel (1.6 wt pct). It appears to be due to a much higher fraction of retained austenite between the polygonal ferrite grains and at the polygonal ferrite/bainite interface in the Nb steel than in the non-Nb steel. This retained austenite has a lower carbon content than that between the bainitic ferrite grains or laths, due to the absence of a second carbon enrichment during the bainite reaction. This distribution of the retained austenite in the Nb steel could be explained by the difference in the morphology of the bainitic structure formed in steels. Since the length of the acicular ferrite laths depends on the grain size,[28] a reduction in the austenite grain size, as in the Nb steel due to NbC precipitation, refines the bainitic ferrite laths in the acicular ferrite. The formation of refined acicular ferrite in the

Nb steel leads to the increase in the internal stress generated during a displacive bainite reaction. This could increase the ability of the retained austenite to remain between the polygonal ferrite grains and at the polygonal ferrite/bainite interface rather than between refined bainitic ferrite laths or grains.

The difference in the distribution of retained austenite before straining in the two steels also leads to the different transformation behaviors of retained austenite during deformation. The retained austenite present between the polygonal ferrite grains tends to transform to martensite at lower strains due to its lower carbon content and, thus, does not improve the elongation of the steel. Furthermore, the retained austenite at the polygonal ferrite/bainite interface also did not contribute much to the elongation of steel due to the nonuniform carbon distribution within the retained austenite crystals and the partial transformation of retained austenite to martensite at lower strains. It is suggested that the part of the retained-austenite crystal in close proximity to the polygonal ferrite has a lower carbon content and transforms to martensite at lower strains, while the areas in close proximity to bainite have a higher carbon content and are more stable. The martensite, formed in the low-carbon region, could propagate the stress to the austenite during further straining and lead to an increase in the transformation rate of the retained austenite. So, the higher amount of retained austenite between the polygonal ferrite grains and at the polygonal ferrite/bainite interface found in the microstructure of the Nb steel could be responsible for the lower uniform elongation of this steel.

The bainite morphology also affects the rate of strain-induced transformation. The formation of a high volume fraction of acicular ferrite, as in the Nb steel, leads to the rapid transformation of some of the retained-austenite crystals to martensite at an early stage of deformation due to the interaction between rigid bainitic ferrite laths and the retained-austenite crystals. On the other hand, the acicular ferrite morphology favors the formation of a high volume fraction of the supersaturated retained austenite due to the geometrical restrictions of the bainitic ferrite laths. The refinement of the acicular ferrite in the Nb steel even increased the tendency for the formation of the supersaturated retained-austenite crystals. During straining, these were further divided, becoming even smaller and more stable. Smaller retained-austenite islands contain lower potential nucleation sites for the transformation to martensite and, consequently, require a greater total driving force for the nucleation of martensite.[9] This could explain why these retained-austenite crystals did not transform to martensite and did not contribute to the increase in the elongation of the Nb steel.

The partial transformation of the retained-austenite crystals between bainitic ferrite found in the Nb steel could be explained not only by the interaction between bainitic ferrite and retained austenite during straining but also by the presence of the defects in the austenite, caused by the lattice distortion due to the interstitial atoms, which increases the strain energy.[29] It is thermodynamically possible for the carbon atoms to move to the defect area and reduce the total strain energy. Consequently, carbon-depleted zones could be formed in austenite,[29] which leads to the partial transformation of the retained austenite crystal during straining. In contrast, the granular bainite, as in the non-Nb steel, stimulates the gradual transformation of the retained austenite to martensite during straining.

A higher amount of coarse blocks of martensite initially present in the microstructure of the Nb steel could also be responsible for its lower elongation. These martensite regions in the Nb steel might be formed during quenching after the 600-second hold at 723 K as a result of insufficient holding time to enrich the retained austenite by carbon. This suggests that the transformation is more sluggish in the steel with Nb and requires more time for completion than in the steel without Nb.

The strain-hardening behavior of the non-Nb and Nb steels reflects the difference in the dynamic of the retained-austenite transformation in these steels (Figure 6). The non-Nb steel demonstrated a gradual variation of strain-hardening rate. This results in the slow transformation of retained austenite to martensite under straining at room temperature, which delays the onset of necking and ultimately leads to the higher uniform and total elongation.[7] A sharp maximum in n, as found in the Nb steel (Figure 6), is evidence of more-rapid transformation of the retained austenite to martensite during straining.[30] This correlates with the lower values of total and uniform elongations found in the Nb steel.

Moreover, the presence of a higher volume fraction of martensite and the formation of the acicular ferrite in the microstructure of the Nb steel affected not only the elongation, but also led to the increase in the yield strength of steel.

In summary, the lower uniform and total elongation of the Nb steel can be explained by the higher amount of retained austenite between the polygonal ferrite grains and at the polygonal ferrite/bainite interface, the higher amount of over-stable retained austenite between bainitic ferrite laths, and the higher amount of martensite formed in the microstructure of the Nb steel before deformation. However, the characteristics of the retained austenite, discussed earlier, do not completely explain the microstructure-property relationships in the TRIP steels.

B. *Role of Polygonal Ferrite and Interaction between Polygonal Ferrite, Retained Austenite, and Martensite during Straining*

The polygonal ferrite in each steel showed a different behavior during straining. The microstructural changes of the polygonal ferrite were observed after ~0.14 strain. For the Nb steel, this strain corresponded to the onset of necking, while at this strain, the strain hardening of the non-Nb steel demonstrated a second maximum (Figure 6). At different stages of straining, the polygonal ferrite grains in the non-Nb steel elongated by almost 2 times more than in the Nb steel. This means that the strain concentrated in the polygonal ferrite matrix and caused it to flow around the bainite and martensite islands. The polygonal ferrite in the Nb steel showed a lower ferrite deformation than in the non-Nb steels and did not flow around the bainitic region during straining. This could be a direct result of the Nb addition promoting precipitation hardening of the ferrite and/or through grain refinement, which leads to the strengthening of ferrite.

One further point, which should be noted, is the higher volume fraction of martensite between the ferrite grains and at the ferrite/bainite interface in the Nb steel. The presence of "as-quenched" martensite in a soft polygonal ferrite matrix led to the formation of a plastic-deformation zone in the polygonal ferrite surrounding the martensite islands (Figure 10). As
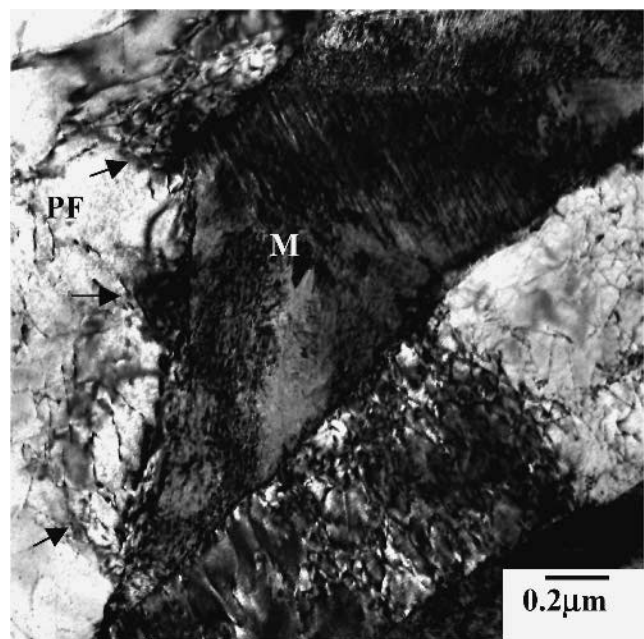

Fig. 10—TEM micrograph (bright-field image) martensite/polygonal ferrite interface before testing. Arrows indicate an increase in the dislocation density in the polygonal ferrite.

reported by Goel *et al.*,[31] this could contribute to an increase in the strain hardening of the polygonal ferrite. In addition, the presence of the hard phase in the soft matrix could increase the strength of the matrix by itself and affect the stress partitioning between the phases. The interaction between the polygonal ferrite and as-quenched martensite during straining also should lead to the formation of an additional plastic-deformation field in the soft matrix that will increase the strain hardening of the polygonal ferrite.

The strain-induced transformation during straining also affected the deformation behavior of the polygonal ferrite. As mentioned previously, the retained austenite present between polygonal ferrite grains and at the polygonal ferrite/bainite interface transformed to martensite at an early stage of deformation. These new strain-induced martensite islands might create extra plastic-deformation zones in the adjacent polygonal ferrite grains due to the volume expansion accompanying the martensite transformation and the new dislocations generated in the polygonal ferrite.[31] This could increase the strain hardening of polygonal ferrite and decrease the mean-stress level within the retained-austenite islands and, through this, delay the austenite-to-martensite transformation. This could be responsible for the presence of coarse untransformed blocks of retained austenite in polygonal ferrite after a 0.1 strain in the Nb steel. Hence, the contribution of polygonal ferrite to the stress-strain behavior during deformation should be considered as interaction between polygonal ferrite, retained austenite, and martensite.

C. *Behavior of Bainite during Straining and Interaction between Bainitic Ferrite, Retained Austenite, and Martensite during Straining*

It was found that the bainite morphology also affects the structure-property relationship in the TRIP steels. Similar to

the polygonal ferrite behavior, the bainitic ferrite of the non-Nb steel also flowed and elongated around the hard martensite islands during straining (up to 95 pct at 0.2 strain). The bainitic ferrite in the Nb steel was more rigid and demonstrated a lower degree of elongation. The higher resistance of bainitic ferrite in the Nb steel to the tensile deformation could be explained by the refinement of the bainitic ferrite laths in the Nb steel. Theoretically, the refinement of the bainitic ferrite laths with different crystallographic orientations should increase the mechanical stability of the retained austenite. As mentioned previously, if the residual austenite is closely surrounded by the relatively rigid and refined bainitic ferrite, the mechanical stability of the retained austenite also increases due to the geometrical restrictions of the bainitic ferrite laths.[32] This also increases the strain hardening of the bainitic ferrite, preventing the elongation of bainite. In addition, the martensite between the bainitic ferrite grains or laths could also strengthen the bainite and affect the overall deformation behavior of this microstructure.

It was observed for the Nb steel that the retained austenite between long, parallel bainitic ferrite laths transforms to martensite at the beginning of straining. Furthermore, the part of the austenite crystal in close proximity to the bainitic ferrite laths transformed faster than the core. This could be due to the rigidity of bainitic ferrite laths caused by the higher level of carbon (by ~0.2 to 0.3 wt pct),[33] the increase in the dislocation density due to the displacive type of transformation, and also by the morphology of the bainitic ferrite. This might stimulate the retained austenite-to-martensite transformation at a low strain due to the concentration of the stress at the interface with its further propagation into the retained austenite crystal during testing in the Nb steel. Thus, the interaction between the bainitic ferrite laths and the retained austenite during straining, on one hand, influences the strain-induced transformation of retained austenite and, on the other hand, affects the behavior of bainite.

The retained austenite with optimum stability, which showed the gradual transformation to martensite during straining, was found in the non-Nb steel within granular bainite. It is suggested that the bainitic ferrite present in the form of grains propagates less stress to the retained austenite during deformation and does not stimulate the rapid transformation of the retained austenite to martensite. Since the non-Nb steel contained the higher amount of granular bainite, it demonstrated the greater elongation.

In summary, due to the complexity of the microstructure, the mechanical properties of the TRIP steels are more dependent on the deformation mode of each phase and the interaction between phases present rather than just the volume fraction and stability of the retained austenite, although this is a function of the surrounding phase morphology.

V.   CONCLUSIONS

The analysis of microstructure-property relationships in thermomechanically processed TRIP steels, with and without Nb, has been conducted. The results have shown that the mechanical properties of the complex multiphase microstructures are determined not only by the strain-induced transformation of retained austenite, but also depend on the characteristics and interactions of all phase present in the microstructure. Both polygonal ferrite and bainite are responsible for a good combination of strength and ductility in the TRIP steels.

Moreover, the morphology of the bainitic ferrite plays a vital role in the retained-austenite stabilization. It has been demonstrated that the coarse blocks of retained austenite located in the polygonal ferrite or at the polygonal ferrite/bainite interface transform to martensite at an early stage of deformation, while the retained austenite present between the bainitic ferrite laths is more stable and can remain in the microstructure even after the testing to failure. This is due to its higher chemical and mechanical stability. The granular bainite, as the dominant second phase, provides the optimum stability of the retained austenite and shows the maximum contribution to the elongation.

REFERENCES

1. Y. Sakuma, O. Matsumura, and H. Takechi: *Metall. Mater. Trans. A*, 1991, vol. 22A, pp. 489-98.
2. S.K. Liu and J. Zhang: *Metall. Mater. Trans. A*, 1990, vol. 21A, pp. 1517-25.
3. V.F. Zackay, E.R. Parker, D. Fahr, and R. Busch: *Trans. ASM*, 1967, vol. 60, pp. 252-59.
4. W.W. Gerberich, P.L. Hemmings, M.D. Merz, and V.F. Zackay: *Trans. Techn. Notes*, 1968, vol. 61, pp. 843-47.
5. O. Matsumura, Y. Sakuma, and H. Takechi: *Trans. Iron Steel Inst. Jpn. Int.*, 1987, vol. 27, pp. 570-79.
6. O. Matsumura, Y. Sakuma, and H. Takechi: *Iron Steel Inst. Jpn. Int.*, 1992, vol. 32 (10), pp. 1100-16.
7. O. Matsumura, Y. Sakuma, and H. Takechi: *Scripta Metall.*, 1987, vol. 21, pp. 1301-06.
8. K. Hulka, W. Bleck, and K. Papamantellos: *Proc. 41st MWSP Conf.*, ISS-AIME, Baltimore, MD, vol. XXXVII, TMS, Warrendale, PA, 1999, pp. 67-76.
9. M.L. Brandt and G.B. Olson: *Ironmaker and Steelmaker*, 1993, vol. 20 (5), pp. 55-60.
10. Y. Tommita: *Mater. Sci.*, 1995, vol. 30, pp. 105-10.
11. G. Reisner, E.A. Werner, P. Kerschbaummaur, I. Papst, and F.D. Fischer: *J. Met.*, 1997, vol. 49 (9), pp. 62-65.
12. M. De Meyer, D. Vanderschueren, and B.C.De Cooman: *Iron Steel Inst. Jpn. Int.*, 1999, vol. 39 (8), pp. 813-22.
13. D.Q. Bai, A. Di Chiro, and S. Yue: *Mater. Sci. Forum*, 1998, vols. 284–286, pp. 253-60.
14. H.C. Chen, H. Era, and M. Shimizu: *Metall. Trans. A*, 1989, vol. 20A, pp. 437-45.
15. V.T.T. Miihkinen and D.V. Edmonds: *Mater. Sci. Technol.*, 1987, vol. 3, pp. 422-30.
16. M. Takahashi and H.K.D.H. Bhadeshia: *Mater. Trans., JIM*, 1991, vol. 32, pp. 689-96.
17. J. Wang and S. Van der Zwaag: *Wire*, 2001, vol. 50, pp. 1527-39.
18. I. Tsukatani, S. Hashimoto, and T. Inoue: *Iron Steel Inst. Jpn. Int.*, 1991, vol. 31 (9), pp. 992-1000.
19. P.J. Jacques, J. Ladrière, and F. Delanny: *Metall. Mater. Trans. A*, 2001, vol. 32A, pp. 2759-68.
20. P. Jacques, A. Petein, and P. Harlet: *Int. Conf. on TRIP-Aided High Strength Ferrous Alloys*, GRIPS Sparking World of Steel, 2002, vol. 1, pp. 281-85.
21. H.K.D.H. Bhadeshia: *Iron Steel Inst. Jpn. Int.*, 2002, vol. 42 (9), pp. 1059-60.

22. *Annual Book of ASTM Standards Metals Test Methods and Analytical Procedures*, 1993, vol. 03.01, E 8, pp. 130-49.
23. G.E. Dieter: *Mechanical Metallurgy*, 2nd ed., McGraw-Hill Book Company, New York, NY, 1988, pp. 87 and 287.
24. B.V. Kovacs: *AFS Trans.*, 1994, vol. 102, p. 417.
25. B.D. Cullity: *Elements of X-Ray Diffraction*, Addison-Wesley Publishing Company, Inc., London, 1978, pp. 411-15.
26. M. Onink, C.M. Brakman, F.D. Tichelaar, E.J. Mittemeijer, S. van der Zwaag, J.H. Root, and N.B. Konyer: *Scripta Metall. Mater.*, 1993, vol. 29 (8), pp. 1011-16.
27. A. Zarei-Hanzaki and S. Yue: *Iron Steel Inst. Jpn. Int.*, 1997, vol. 37 (6), pp. 583-89.
28. I.B. Timokhina, P.D. Hodgson, and E.V. Pereloma: *Metall. Trans. A*, 2003, vol. 34A, pp. 1599-609.
29. M.X. Zhang and P.M. Kelly: *Mater. Characterization*, 1998, vol. 40, pp. 159-68.
30. P.J. Evans, L.K. Crawford, and A. Jones: *Ironmaking and Steelmaking*, 1979, vol. 24 (5), p. 361.
31. N.C. Goel, S. Sangal, and K. Tangri: *Metall. Trans. A*, 1985, vol. 16, pp. 2013-22.
32. V.T.T. Miihkinen and D.V. Edmonds: *Mater. Sci. Technol.*, 1987, vol. 3, pp. 422-30.
33. H.K.D.H. Bhadeshia and D.V. Edmonds: *Metall. Trans. A*, 1979, vol. 10, pp. 895-907.